Advances in Medical Sciences 66 (2021) 326–335

Contents lists available at ScienceDirect

Advances in Medical Sciences

journal homepage: www.elsevier.com/locate/advms

Original research article

Serum and urine analysis with gold nanoparticle-assisted laser desorption/ionization mass spectrometry for renal cell carcinoma metabolic biomarkers discovery

Adrian Arendowski [a,b,*], Krzysztof Ossoliński [c], Anna Ossolińska [c], Tadeusz Ossoliński [c], Joanna Nizioł [b], Tomasz Ruman [b]

[a] Institute of Medical Studies, Medical College, University of Rzeszow, Rzeszow, Poland
[b] Faculty of Chemistry, Rzeszow University of Technology, Rzeszow, Poland
[c] Department of Urology, John Paul II District Hospital, Kolbuszowa, Poland

ARTICLE INFO

Keywords:
Gold nanoparticles
Kidney cancer biomarkers
Laser desorption/ionization
Mass spectrometry
Renal cell carcinoma

ABSTRACT

Purpose: Renal cell carcinoma (RCC) is a very aggressive and often fatal heterogeneous disease that is usually asymptomatic until late in the disease. There is an urgent need for RCC specific biomarkers that may be exploited clinically for diagnostic and prognostic purposes.
Materials/methods: Serum and urine samples were collected from patients with diagnosed kidney cancer and assessed with gold nanoparticle enhanced target (AuNPET) surface assisted-laser desorption/ionization mass spectrometry (SALDI MS) based metabolomics and statistical analysis.
Results: A database search allowed providing assignment of signals for the most promising features with a satisfactory value of the area under the curve and accuracy. Four potential biomarkers were found in urine and serum samples to distinguish clear cell renal cell carcinoma (ccRCC) from controls, 4 for the ccRCC with and without metastases, and 6 metabolites to distinguish low and high stages or grades.
Conclusions: This pilot study suggests that serum and urine metabolomics based on AuNPET-LDI MS may be useful in distinguishing types, grades and stages of human RCC.

1. Introduction

Kidney cancers are the 16th most frequently diagnosed types of cancer. Worldwide, in the year 2018, there were more than 403 thousand new cases of kidney cancer, which is 2.2% of all cancers and up to 175 thousand deaths due to this disease [1]. Approximately 80% of adult kidney cancers are renal cell carcinomas (RCCs) [2]. They are a heterogeneous group of tumors classified by WHO into several subtypes: clear cell (80% of cases), papillary (10%), chromophobe (5%), medullary and collecting duct (below 1%) and other unclassified subtypes (~5%) [3]. RCC develops asymptomatically for a long time and is often detected in advanced stages, approximately 20% of patients have metastases at the time of diagnosis [4]. Kidney tumors are usually detected by incidental medical imaging methods, but imaging cannot distinguish neither histopathological type of cancer nor its grade. For that reason, RCC still remains a major challenge and forces searching for diagnostic and prognostic procedures [5,6]. Renal mass biopsy may be helpful but is prone to sampling error and ultimately is invasive and associated with some morbidity [7,8]. That being the case, it is important to develop non-invasive methods, for example, based on distinctive chemical compounds from bioliquids, called biomarkers, that might indicate a development of tumor.

Biomarkers can be genes [9], proteins [10] and metabolites [11], but proteomic approach dominates in current strategies of cancer biomarker search. Several RCC protein biomarkers have been proposed, but they suffer from low sensitivity and specificity [12]. Cancer is a disease that alters cell metabolism, so it seems that the appropriate approach will be the metabolic profiling [8,13].

In the case of RCC, researchers report that mutations affecting hypoxia inducible factor (HIF), succinate dehydrogenase and fumarate hydratase alter cellular metabolism and contribute to cancer cellular growth [14]. The major metabolic disorders associated with kidney cancer occur in amino acid and fatty acid metabolism, glycolysis and also tricarboxylic acid (TCA) cycle [15]. Due to the location of RCC in

* Corresponding author. Institute of Medical Studies, Medical College, University of Rzeszow, Warzywna 1a, 35-310, Rzeszow, Poland.
E-mail address: adrian@arendowski.hub.pl (A. Arendowski).

https://doi.org/10.1016/j.advms.2021.07.003
Received 1 April 2021; Received in revised form 2 June 2021; Accepted 6 July 2021

proximity to the urinary collecting system and blood circulation it is suggested that analysis of serum and urine is the best suited for screening to detect metabolic biomarkers of this tumor. Metabolomic approach has already been applied to analyze tissue [16–19], plasma [20,21], serum [22–25] and urine [26–29] samples from RCC patients. Most of this research is focused on distinguishing between RCC and disease-free controls, often without assessing cancer type, grades and stages. An exception is the work by Gao et al. [30] using proton magnetic resonance (^{1}H NMR), which distinguished between patients with and without metastases, and work by Falegan et al. [8], in which the authors used ^{1}H NMR and gas chromatography coupled to mass spectrometry (GC-MS) to differentiate between benign and metastatic renal masses, as well as between low grade and high grade RCC. Additionally, recent studies using NMR and laser mass spectrometry on monoisotopic silver-109 nanoparticles enhanced target (^{109}AgNPET), distinguished between benign and metastatic cancer as well as the grades of RCC in urine [31], serum [25] and tissue [32] samples.

Mass spectrometry (MS) is the predominantly used family of analytical methods in cancer biomarker research mainly due to its high resolution and sensitivity compared to other techniques. Among the various MS methods of ionization, matrix-assisted laser desorption/ionization (MALDI) technique deserves special attention. The process of preparing a sample for MALDI MS measurements consists of mixing the analyte with a compound with strong light absorption in the range of waves emitted by the laser. This compound, called a matrix, is most often a low molecular weight organic acid such as α-cyano-4-hydroxycinnamic acid (CHCA) and 2,5-dihydroxybenzoic acid (DHB). The matrix particles excited by the laser beam pulse mediate the ionization of the analyte molecules. MALDI is mainly used for analyzing peptides and proteins [33], nucleic acids [34] and synthetic polymers [35]. Due to the soft ionization process, high mass determination accuracy and very high sensitivity over a wide mass range, this method is among the best choices for biological material analysis. MALDI MS method has already been used as a tool for peptide and protein profiling for RCC [36]. However, MALDI spectra contain a high chemical background below m/z 800 due to the use of organic matrices. For small molecules, such as metabolites, surface-assisted laser desorption/ionization (SALDI) [37] solutions, based on various types of nanostructures, are generally better suited. As the literature search proves, gold nanostructures are among the most frequently used for laser MS [38]. An example of the use of gold nanoparticles (AuNPs) in SALDI is the work of Liu et al. [39], in which AuNPs of various sizes covered with ligands were tested for the analysis of low molecular weight compounds. Gold nanoparticles have also been used in SALDI MS in combination with other materials such as silver [40,41] or carbon nanodots, which has been applied to SALDI technique for cytosensing of metals for cancer cells [42]. Several studies present the advantages of gold-nanoparticle enhanced target (AuNPET) for laser desorption/ionization mass spectrometry analysis and imaging of low molecular weight (LMW) compounds of different polarity in complex biological mixtures [43,44], also in kidney cancer tissue [45], and more recently, for metabolomic screening of serum [46] and urine [47] samples of patients with diagnosed RCC and statistical comparison with control group of samples of healthy volunteers in order to discover new diagnostic biomarker candidates. Compared to commonly used MALDI MS, this method has been proven to produce much lower chemical background, allow much more precise internal calibration and be better for medium and low polar compounds. The comparison of the AuNPET method with other methods is presented in Table 1. It should be noted that some of the methods mentioned in Table 1 apply acidic sample solution or acidic eluent. In this case, it is possible that some of acid-labile compounds may be hydrolyzed, for example, it was shown that proteins and peptides may undergo hydrolytic breakdown on the level of sample preparation in MALDI [48].

The aim of this study is to demonstrate the capabilities of AuNPET LDI MS method as a tool for distinguishing the types, grades and stages of RCC. For this purpose, we used gold nanoparticle-enhanced target laser desorption/ionization mass spectrometry in metabolomics analyses of serum and urine samples with statistical analysis to investigate if metabolic profiles could differentiate between clear cell renal cell carcinoma (ccRCC) and other types, with and without metastases, low stages (T1 and T2) versus high stages (T3 and T4) and also low grade (Fuhrman I and II) versus high grade (Fuhrman III and IV).

2. Materials and methods

2.1. Participants

Serum and urine samples were obtained from 50 patients with diagnosed kidney cancer. Patient who agreed to participate in the study donated 50 mL of urine and 10 mL of blood according to standard medical procedure. Patient characteristics are provided in Table 2. The

Table 2
Clinical characteristics of patients.

		ccRCC patients	others renal tumors patients
Total		33	17
Age (years)		35–89	43–84
Mean		69	66
Sex	Male	18	12
	Female	15	5
Stage (T)	T1	21	12
	T2	1	2
	T3	10	0
	T4	1	0
	undefined	0	3
Nodes (N)	N0	32	14
	N1	1	0
	undefined	0	3
Metastases (M)	M0	29	13
	M1	4	1
	undefined	0	3
Grade (Fuhrman)	I	6	1
	II	15	2
	III	10	3
	IV	2	0
	undefined	0	11

Table 1
Comparison of analytical methods used to detect RCC biomarkers.

Method	AuNPET	^{109}AgNPET	MALDI	LC-MS/MS	GC-MS	NMR
LOD	up to amol/spot	up to amol/spot	up to fmol/spot	up to amol	up to fmol	up to nmol
Suitable for LMW compounds	yes	yes	no	yes	yes	yes
Typical sample volume	0.2 μL	0.2 μL	0.2 μL	1–10 μL	1–10 μL	0.6 mL
Sample preparation time	20–30s	20–30s	30–60s	10–60 min	10–20 min	1–3 min
Analysis time per sample	5–20s	5–20s	5–20s	10–30 min	10–60 min	10–300 min
Acidic sample conditions	no	no	yes	yes	no	no
References	[46,47],	[25,31],	[36]	[28,29],	[8,18],	[20,21,30],

Abbreviations: ^{109}AgNPET – silver-109 nanoparticle-enhanced target, AuNPET – gold nanoparticle-enhanced target, GC – gas chromatography, LC - liquid chromatography, LMW – low molecular weight, LOD – limit of detection, MALDI – matrix-assisted laser desorption/ionization, MS – mass spectrometry, NMR – nuclear magnetic resonance, RCC – renal cell carcinoma.

control group consisted of fifty healthy volunteers who donated 10 mL of blood and 50 mL of urine, for which the presence of kidney or bladder tumors had been excluded by abdominal ultrasound. The average age was 51 years old and the male to female ratio was 3:2.

2.2. Ethical issues

All experiments were performed in compliance with the local laws and institutional guidelines (Rzeszów University of Technology biological material guidelines). The samples' and clinical data collection and analysis, were performed in accordance with the approval of the local bioethics committee of the University of Rzeszów, Poland (no. 2018/04/10). All patients gave their written informed consent for providing samples and clinical data.

2.3. Methods

As a precursor for nanoparticle synthesis we used chloro(trimethylphosphite)gold(I) of 97+% purity (Sigma-Aldrich, Saint Louis, MO, USA). The borane pyridine complex (BH3:py) used as a reducing agent was at ~8 M borane concentration (Sigma-Aldrich, Saint Louis, MO, USA). All solvents were of High Performance Liquid Chromatography (HPLC) quality and were purchased from Sigma-Aldrich, except for 18 MΩ water which was produced locally. Magnetic stainless steel plate of H17 grade was made locally and used with Bruker NALDI adapter (Bruker Daltonik GmbH, Bremen, Germany).

2.4. Preparation of AuNPET target

The AuNPET was prepared in a similar manner to that described in a recent publication [49]. Stainless steel plate of 45x35 mm size was inserted into a large Petri dish containing chloro(trimethylphosphite) gold(I) (25 mg) dissolved in acetonitrile (50 mL). To this solution, 8 M BH3:py complex in pyridine (173 μL) was added. After 48 hours of reaction, target plate was washed several times with acetonitrile, wiped with cotton wool ball and washed three times with acetonitrile and deionized water.

2.5. Sample preparation

Obtained urine and serum samples were immediately frozen and stored at −60 °C. Prior to measurements, an unfreezing step was performed in room temperature, followed by 500-times dilution with ultrapure water for serum and 1000-times for urine. Volumes of 0.5 μL of samples solutions were placed directly on target plate, air dried and inserted into MS apparatus for measurements.

2.6. LDI MS experiment

Laser desorption/ionization mass spectrometry experiments were performed using Bruker Autoflex Speed Time-of-Flight mass spectrometer (Bruker Daltonik GmbH, Bremen, Germany) equipped with a SmartBeam II laser (355 nm wavelength) in positive-ion reflectron mode. Spectra were recorded in the *m/z* range of 80–2000, with ions below *m/z* 79 deflected from the flight trajectory. Laser impulse energy was approximately 100–190 μJ and laser repetition rate was 1 kHz. Number of laser shots was 20,000 (4x5000 shots) for each sample spot. The operating conditions voltages were as follows: ion source 1: 19 kV; ion source 2: 16.7 kV; reflector 1: 21 kV; reflector 2: 9.55 kV. The spectra were calibrated with FlexAnalysis (version 3.3; Bruker Daltonik GmbH, Bremen, Germany) using enhanced cubic calibration model and analyzed with mMass 5.5.0-open source program [50]. Mass calibration was performed on 5 points using internal standards (gold ions and clusters from Au^+ to Au_5^+). Reproducibility was tested by measuring triplicates and comparing signals intensities for *m/z* values for ions: Au^+ to Au_5^+ for 10 cancer and 10 normal samples. All intensities were within 20% of mean value.

2.7. Data analysis

Database search of chemical compounds was carried out using a custom made program for Human Metabolome Database (HMDB) [51] and LIPID MAPS tools [52]. Theoretical *m/z* values were confirmed by using ChemCalc program available online [53]. Statistical analysis of results was performed with the use of MetaboAnalyst 5.0 service [54]. Data was normalized by sum, cube root transformed, and default Pareto scaling was used. For creating receiver operating characteristic (ROC) curve random forests has been chosen as classification method and Random Forest was selected as feature ranking method.

3. Results and discussion

The goal of our research was to find metabolites present in serum and urine that could be biomarkers for distinguishing types, stages and grades of RCC. For this purpose, 50 samples of serum and urine from patients with diagnosed kidney cancer and 50 samples from healthy volunteers were assessed using AuNPET. Obtained spectra from patients and controls were compared using MetaboAnalyst 5.0 [54]. Among patients diagnosed with renal cancer, 33 had ccRCC, of which 29 had no metastases, and 4 had metastases (Table 2). The urine and serum samples were stratified by pathological stage - 22 from ccRCC low stages (T1 and T2) patients and 11 from ccRCC high stages (T3 and T4) patients, 21 from ccRCC low grade (Fuhrman I and II) patients and 12 from ccRCC high grade (Fuhrman III and IV) patients.

The peak intensity data from LDI MS spectra of serum and urine was subjected to multivariate data analysis, and two-dimensional score plots of the Orthogonal Partial Least Squares–Discriminant Analysis (2D-OPLS-DA) (Figs. 1 and 2) as well as Partial Least Squares–Discriminant Analysis (2D-PLS-DA) (Supplementary Figs. 1 and 2) score plots were generated for the entire data set. Analysis of PLS-DA results obtained for serum samples (Supplementary Fig. 1) shows that only for the comparison of ccRCC with and without metastases it was possible to obtain complete separation of the groups. When the OPLS-DA statistical method was used for analysis of the blood serum mass spectra (Fig. 1), the group separation was obtained for no metastases and metastases, as well as, for ccRCC samples and the control group. When analyzing Supplementary Fig. 2, presenting PLS-DA results of urine mass spectrometry data, it can be concluded that, as with serum samples, complete group separation is visible for ccRCC with and without metastases, but results from OPLS-DA (Fig. 2) show complete discrimination for no metastases and metastases, low and high stages ccRCC, as well as for low and high grade. The obtained results suggest that serum and urine analyses based on the AuNPET LDI MS method can be used to identify metabolic differences between groups.

Based on the PLS-DA and OPLS-DA statistical methods, we obtained the *m/z* values that had the greatest impact on group separation. Only features for which the variable importance in projection (VIP) scores were ≥1 and value $|p(corr)[1]| \geq 0.5$, were taken into account. Mass features were assigned using HMDB with $|\Delta m/z| \leq 15$ ppm which allowed for listing 12 potential biomarkers from serum (Table 3) and 8 potential biomarkers from urine (Table 4).

3.1. Serum samples analysis

In Fig. 3, we present box plots based on ANOVA statistical method for each of *m/z* values from the blood serum samples, ROC curves for these *m/z* values are presented in Supplementary Fig. 3. For *m/z* values from the urine samples box plots are presented in Fig. 4 and ROC curves in Supplementary Fig. 4. In Figs. 3 and 4, we present the changes in signal intensities in the compared data sets as well as in comparison with the control group.

Two features were found in the serum samples that distinguished patients with ccRCC from patients with other types of renal tumors and the control group (Table 3). It was the *m/z* value of 398.2302 (Fig. 3A,

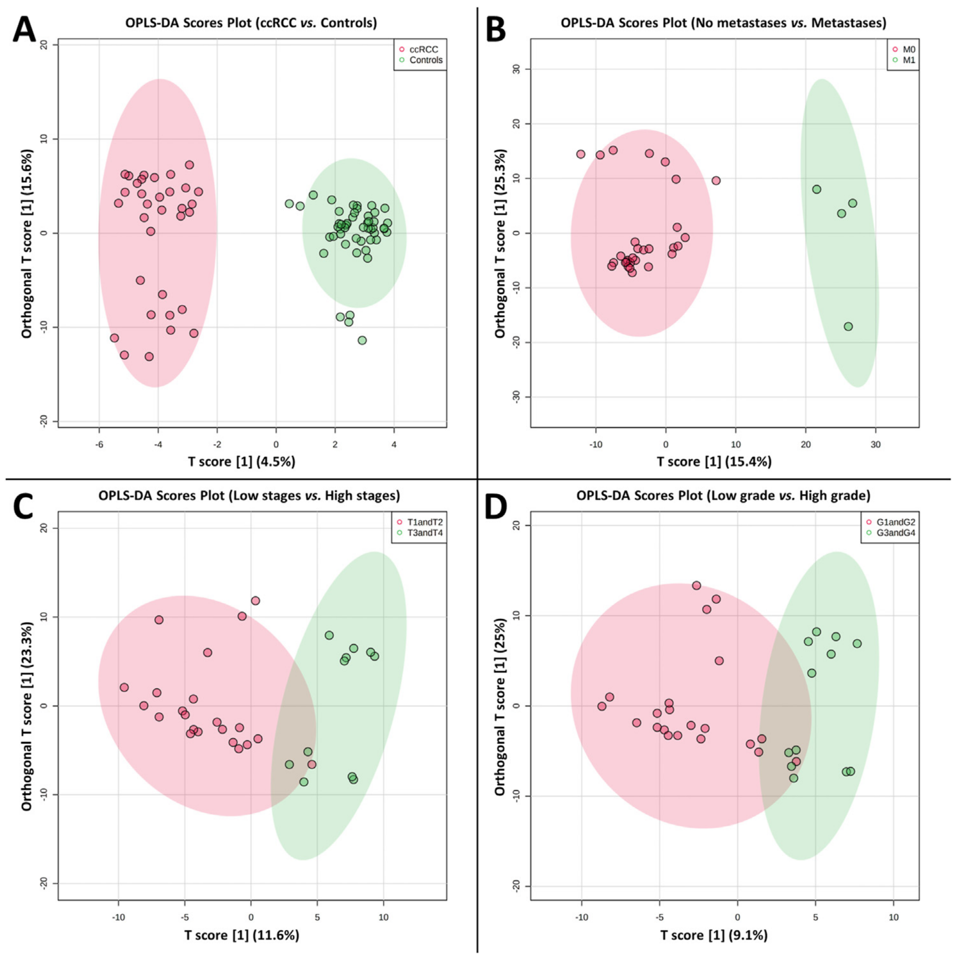

Fig. 1. Graphical representation of OPLS-DA statistical analysis of MS data from blood serum samples: ccRCC vs. controls (A), without metastases (M0) ccRCC vs. with metastases (M1) ccRCC (B), low stages (T1 and T2) ccRCC vs. high stages (T3 and T4) ccRCC (C), low grade (G1 and G2) ccRCC vs. high grade (G3 and G4) ccRCC (C). *Abbreviations*: ccRCC – clear cell renal cell carcinoma, MS - mass spectrometry, OPLS-DA - orthogonal projections to latent structures discriminant analysis.

Supplementary Fig. 3A) that was assigned to 2-hydroxylauroylcarnitine, and the value of 409.1584 (Fig. 3B, Supplementary Fig. 3B) that was assigned to melatonin glucuronide. Both metabolites were upregulated in the blood serum samples from patients with ccRCC and had an area under the curve (AUC) above 0.7. Accuracy of the test based on 2-hydroxylauroylcarnitine is equal to 71.1% (Supplementary Fig. 5A) and on melatonin glucuronide 65.1% (Supplementary Fig. 5B). AUC of the model based on the two proposed biomarkers is 0.775 and accuracy of this model is equal to 71% (Supplementary Fig. 6A and 6B). 2-Hydroxylauroylcarnitine and melatonin glucuronide, have already been reported as potential blood kidney cancer biomarkers [46]. Melatonin glucuronide is a metabolite of melatonin, a naturally occurring compound found in animals [51]. 2-Hydroxylauroylcarnitine belongs to a group of chemicals called acyl carnitines, which have a higher concentration in the urine and tissue of renal cancer patients compared to the control group [29,55].

Three serum biomarkers have been proposed to distinguish between ccRCC with and without metastases, i.e. triglycerides (TGs) of the ion formula $[C_{53}H_{100}O_5{+}K]^+$ and $[C_{55}H_{100}O_5{+}K]^+$, as well as phosphatidylcholine PC(42:0). All molecules showed higher intensity in the samples from patients diagnosed with metastatic ccRCC, however the intensity in the samples from patients without metastases was higher than in the controls but lower than that in patients with metastases (Fig. 3C, D, 3E). Two metabolites, TG(52:4) and PC(42:0), have already been considered as biomarkers for kidney cancer [46]. Based on our recent publications [29,45], it can be concluded, that the change of lipid content is an important feature of RCC. Studies have shown, that kidney tumor tissue contains twice the amount of phosphatidylcholines (PCs) compared to normal tissue [56]; and additionally, TG presence in RCC is critical for sustained tumorigenesis, but tumor cell viability is not completely understood [57]. For TG(50:2), AUC is equal to 0.810 and is the highest among all the proposed biomarkers (Supplementary Fig. 3C), for the other two molecules, the AUC is above 0.7. The accuracy for the test, based on all three proposed biomarkers, has been calculated and is 60.6% (Supplementary Fig. 6D).

The m/z values of 203.0598, 204.0616 and 207.0192 are proposed to distinguish between low (T1 and T2) and high (T3 and T4) stages of ccRCC samples. All signals have higher intensity in the samples with T3 and T4 stages of ccRCC than in the samples with low stages (Fig. 3F–H). AUC for all features is 0.617 and accuracy of the test is 57.6% (Supplementary Fig. 6E and 6F). Experimental m/z 204.0616 and 207.0192 have been assigned to tyrosine and 2,3-diaminosalicylic acid, respectively, metabolites considered as potential renal cancer biomarkers in another study [46]. The AUC for these two features is slightly above 0.5 (Supplementary Fig. 3G and 3H) and is lower than that observed in the cited study [46]. The explanation for this observation may be, that the ccRCC samples with low and high stages are more similar from a molecular point of view than the kidney cancer and control samples that were compared in the previous publication [46]. Cross validation accuracy of the test based on tyrosine is low and amounts to 42.4% (Supplementary Fig. 5G), in contrast to the 2,3-diaminosalicylic acid based test where it is 72.7% (Supplementary Fig. 5H). Metabolite whose potassium adduct has been attributed m/z 203.0598 is kynuramine. This potential biomarker for RCC stages has AUC equal to 0.657 (Supplementary Fig. 3F) and test accuracy of 63.6% (Supplementary Fig. 5F). The expression of

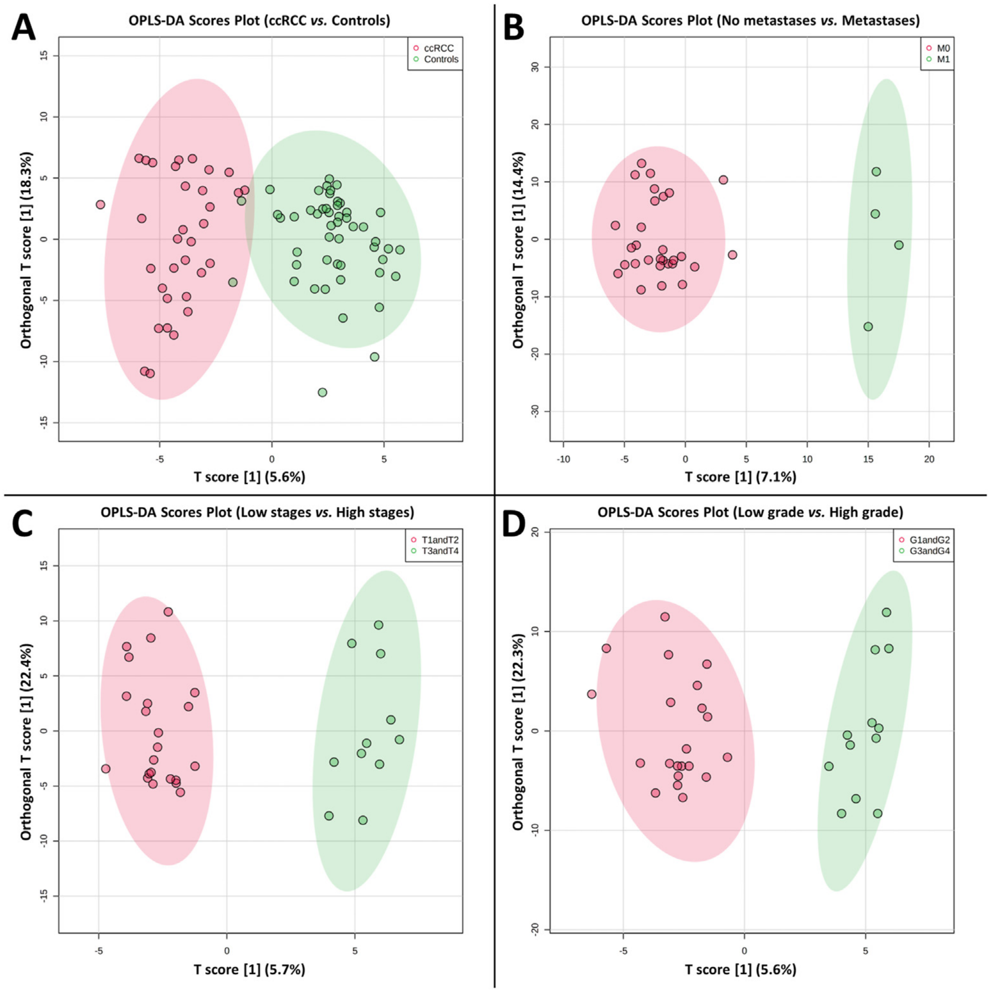

Fig. 2. Graphical representation of OPLS-DA statistical analysis of MS data from urine samples: ccRCC vs. controls (A), without metastases (M0) ccRCC vs. with metastases (M1) ccRCC (B), low stages (T1 and T2) ccRCC vs. high stages (T3 and T4) ccRCC (C), low grade (G1 and G2) ccRCC vs. high grade (G3 and G4) ccRCC (C). *Abbreviations*: ccRCC – clear cell renal cell carcinoma, MS - mass spectrometry, OPLS-DA - orthogonal projections to latent structures discriminant analysis.

Table 3
List of ions and compounds found by statistical analysis of blood serum samples mass spectra.

Metabolite	Ion formula	Experimental *m/z*	Calculated *m/z*	Δ*m/z* [ppm]	Reg.[a]	AUC[b]	Accuracy [%]	VIP[c]	p(corr)[1][d]	Fig.
ccRCC vs. Control										
2-Hydroxylauroylcarnitine	$[C_{19}H_{37}NO_5+K]^+$	398.2302	398.2303	−0.3	↑	0.765	71.1	1.4	−0.56	3A
Melatonin glucuronide	$[C_{19}H_{24}N_2O_8+H]^+$	409.1584	409.1605	−5.1	↑	0.714	65.1	1.4	−0.53	3B
ccRCC without metastases vs. ccRCC with metastases										
TG(50:2)	$[C_{53}H_{100}O_5+K]^+$	855.7082	855.7202	−14.0	↓	0.810	60.6	1.8	0.53	3C
TG(52:4)	$[C_{55}H_{100}O_5+K]^+$	879.7081	879.7202	−13.8	↓	0.746	60.6	1.4	0.50	3D
PC(42:0)	$[C_{50}H_{102}NO_7P + Na]^+$	882.7268	882.7286	−2.0	↓	0.759	66.7	1.5	0.51	3E
Low stages (T1 and T2) ccRCC vs. High stages (T3 and T4) ccRCC										
Kynuramine	$[C_9H_{12}N_2O + K]^+$	203.0598	203.0581	8.4	↓	0.657	63.6	1.5	0.58	3F
Tyrosine	$[C_9H_{11}NO_3+Na]^+$	204.0616	204.0631	−7.4	↓	0.537	42.4	1.1	0.52	3G
2,3-Diaminosalicylic acid	$[C_7H_8N_2O_3+K]^+$	207.0192	207.0167	12.1	↓	0.529	72.7	1.2	0.57	3H
Low grade (Fuhrman I and II) ccRCC vs. High grade (Fuhrman III and IV) ccRCC										
Kynuramine	$[C_9H_{12}N_2O + K]^+$	203.0598	203.0581	8.4	↓	0.702	57.6	1.9	0.54	3I
2,3-Diaminosalicylic acid	$[C_7H_8N_2O_3+K]^+$	207.0192	207.0167	12.1	↓	0.631	57.6	1.0	0.50	3J
2-Hydroxylauroylcarnitine	$[C_{19}H_{37}NO_5+K]^+$	398.2307	398.2303	1.0	↑	0.663	60.6	1.1	−0.51	3K
TG(52:4)	$[C_{55}H_{100}O_5+K]^+$	879.7081	879.7202	−13.8	↓	0.645	63.6	2.4	0.59	3L

[a] Regulation of the intensity in samples.
[b] Area under the ROC curve.
[c] VIP score obtained on the basis of PLS-DA analysis.
[d] p(corr) [1] value obtained on the basis of OPLS-DA analysis.

indoleamine 2,3-dioxygenase, the enzyme involved in the metabolism of L-tryptophan or melatonin to kynuramines, can be found in most, both normal and cancerous, human cells. Moreover, some studies have shown a correlation between increased expression of this enzyme and significant shortening of survival expectation of cancer patients [58]. This would explain the increase of the kynuramine signal intensity in samples with

Table 4
List of ions and compounds found by statistical analysis of urine samples mass spectra.

Metabolite	Ion formula	Experimental m/z	Calculated m/z	Δm/z [ppm]	Reg.[a]	AUC[b]	Accuracy [%]	VIP[c]	p(corr) [1][d]	Fig.
ccRCC vs. Control										
9,12,13-Trihydroxyoctadecenoic acid	$[C_{18}H_{34}O_5+Na]^+$	353.2263	353.2298	−9.9	↑	0.659	63.9	1.3	0.51	4A
3-Hydroxydecanoyl carnitine	$[C_{17}H_{33}NO_5+Na]^+$	354.2297	354.2251	13.0	↑	0.663	65.1	1.3	0.50	4B
ccRCC without metastases vs. ccRCC with metastases										
Uridine 3′-monophosphate	$[C_9H_{13}N_2O_9P + H]^+$	325.0459	325.0431	8.6	↓	0.776	72.7	2.6	0.53	4C
Low stages (T1 and T2) ccRCC vs. High stages (T3 and T4) ccRCC										
Indole-3-acetylglycine	$[C_{12}H_{12}N_2O_3+K]^+$	271.0439	271.0479	−14.8	↓	0.653	60.6	1.8	0.59	4D
Urothion	$[C_{11}H_{11}N_5O_3S_2+H]^+$	326.0424	326.0376	14.7	↓	0.715	66.7	1.4	0.51	4E
Myo-inositol 1,4-bisphosphate	$[C_6H_{14}O_{12}P_2+H]^+$	341.0084	341.0033	15.0	↓	0.665	66.7	2.3	0.50	4F
Low grade (Fuhrman I and II) ccRCC vs. High grade (Fuhrman III and IV) ccRCC										
Indole-3-acetylglycine	$[C_{12}H_{12}N_2O_3+K]^+$	271.0439	271.0479	−14.8	↓	0.806	69.7	2.3	0.66	4G
Phenylacetylglutamine	$[C_{13}H_{16}N_2O_4+Na]^+$	287.1003	287.1002	0.3	↓	0.790	69.7	1.2	0.50	4H

[a] Regulation of the intensity in samples.
[b] Area under the ROC curve.
[c] VIP score obtained on the basis of PLS-DA analysis.
[d] p(corr) [1] value obtained on the basis of OPLS-DA analysis.

high-stage ccRCC. This metabolite has not yet been reported as a biomarker for ccRCC.

To distinguish low-from high-grade ccRCC, four *m/z* values were determined. All metabolites assigned to peaks have already been described in the present study as potential serum biomarkers for various types and stages of ccRCC. They are adducts of kynuramine, 2,3-diaminosalicylic acid, 2-hydroxylauroylcarnitine and triglyceride TG(52:4) (Table 3). For three features, an increase in the intensity was observed in the high-grade (Fuhrman III and IV) ccRCC samples; only for 2-hydroxylauroylcarnitine the signal intensity was increased in the low-grade ccRCC samples (Fig. 3K). For all the proposed biomarkers, the AUC was over 0.6, and the largest AUC was recorded for kynuramine - 0.702 (Supplementary Fig. 3I). For the test based on all four compounds, the AUC was 0.731 and the accuracy was 75.8% (Supplementary Fig. 6G and 6H).

3.2. *Urine samples analysis*

Two urine biomarkers have been proposed to distinguish patients with ccRCC from patients with other types of renal tumors and the control group (Table 4). It was the 9,12,13-trihydroxyoctadecenoic acid for *m/z* 353.2263 (Fig. 4A) and 3-hydroxydecanoyl carnitine for *m/z* 354.2297 (Fig. 4B). Both signals have higher intensity in the ccRCC samples than in the controls, but the intensity is lower than in other types of renal tumors. The AUC for both features is above 0.65 (Supplementary Fig. 4A and 4B). Accuracy of the test based on 9,12,13-trihydroxyoctadecenoic acid was 63.9% (Supplementary Fig. 7A), for 3-hydroxydecanoyl carnitine it was 65.1% (Supplementary Fig. 7B), and for the test based on the two proposed urine biomarkers the AUC was 0.623 and accuracy was 61.4% (Supplementary Fig. 8A and 8B). 9,12,13-trihydroxyoctadecenoic acid has already been reported as a potential urine renal cancer biomarker [47]. 3-hydroxydecanoyl carnitine has not been previously considered as a biomarker for RCC, but this metabolite belongs to the group of acyl carnitines compounds that have been repeatedly reported as markers of kidney cancer [29,55].

To distinguish between the ccRCC patients with and without metastases one feature was found which was assigned to the proton adduct of uridine 3′-monophosphate. This metabolite was down-regulated in the urine samples from ccRCC patients without metastases (Fig. 4C) and had the AUC equal to 0.776 (Supplementary Fig. 4C). The accuracy of the test was 72.7% (Supplementary Fig. 7C).

Three features were found in the urine samples that distinguished between the low- and high-stage ccRCC. The *m/z* values of 271.0439, 326.0424 and 341.0084 were assigned to indole-3-acetylglycine, urothion and myo-inositol 1,4-bisphosphate, respectively. For all features, an increase in the intensity was found in high-stage ccRCC. The accuracy of the test for *m/z* 341.0084 and 326.0424 was 66.7% (Supplementary Fig. 7E and 7F) and for indole-3-acetylglycine 60.6% (Supplementary Fig. 7D). The AUC for all features was over 0.65 (Supplementary Fig. 4D, E and F). For the test based on all three compounds, the AUC was 0.602 and the accuracy was 60.6% (Supplementary Fig. 8C and D). None of these metabolites have been considered as a renal tumor biomarker, but the urothion belongs to a group called pterins that have been studied extensively as putative urine biomarkers for early cancer detection and diagnosis [59] inter alia in bladder cancer [60]. Myo-inositol 1,4-bisphosphate is a metabolite of myo-inositol belonging to inositol phosphates, which play an important role in cellular functions, such as growth, apoptosis and cell migration, and furthermore, myo-inositol has already been considered as a potential biomarker for RCC [31,61].

The *m/z* values of 271.0439 and 287.1003 are proposed to distinguish between low (Fuhrman I and II) and high (Fuhrman III and IV) grades of ccRCC urine samples. All signals had higher intensity in the samples with Fuhrman III and IV grades than in the samples with low grades (Fig. 4G–H). The AUC for all features was 0.817 and the accuracy of the test was 78.8% (Supplementary Fig. 8E and F). A potassium adduct of indole-3-acetylglycine was assigned to *m/z* 271.0439. This metabolite showed the highest AUC among the proposed urinary biomarkers - 0.806 (Supplementary Fig. 4G). The other metabolite, phenylacetylglutamine, also had a high AUC of 0.79 (Supplementary Fig. 4H). This compound occurs naturally in human urine. Higher levels of phenylacetylglutamine have also been found in patients with gastric cancer and Lario et al. [62] concluded that this may indicate deregulation of phenylalanine or glutamine metabolism.

4. Conclusions

AuNPET-SALDI-MS was used for analysis of serum and urine samples from 33 patients with diagnosed ccRCC and 50 healthy volunteers. The methodology allowed for the identification of down- and upregulated 8 features in the blood serum and 7 in the urine samples that could potentially serve as ccRCC biomarkers. We found 4 potential biomarkers, in both types of samples, that distinguish ccRCC from healthy controls, 4 that distinguish between the ccRCC with and without metastases, 6 metabolites that distinguish low (T1 and T2) from high (T3 and T4) stages, and 6 that distinguish low (Fuhrman I and II) from high (Fuhrman III and IV) grades of ccRCC. These tools can be potentially employed clinically to identify types, grades and stages of RCC.

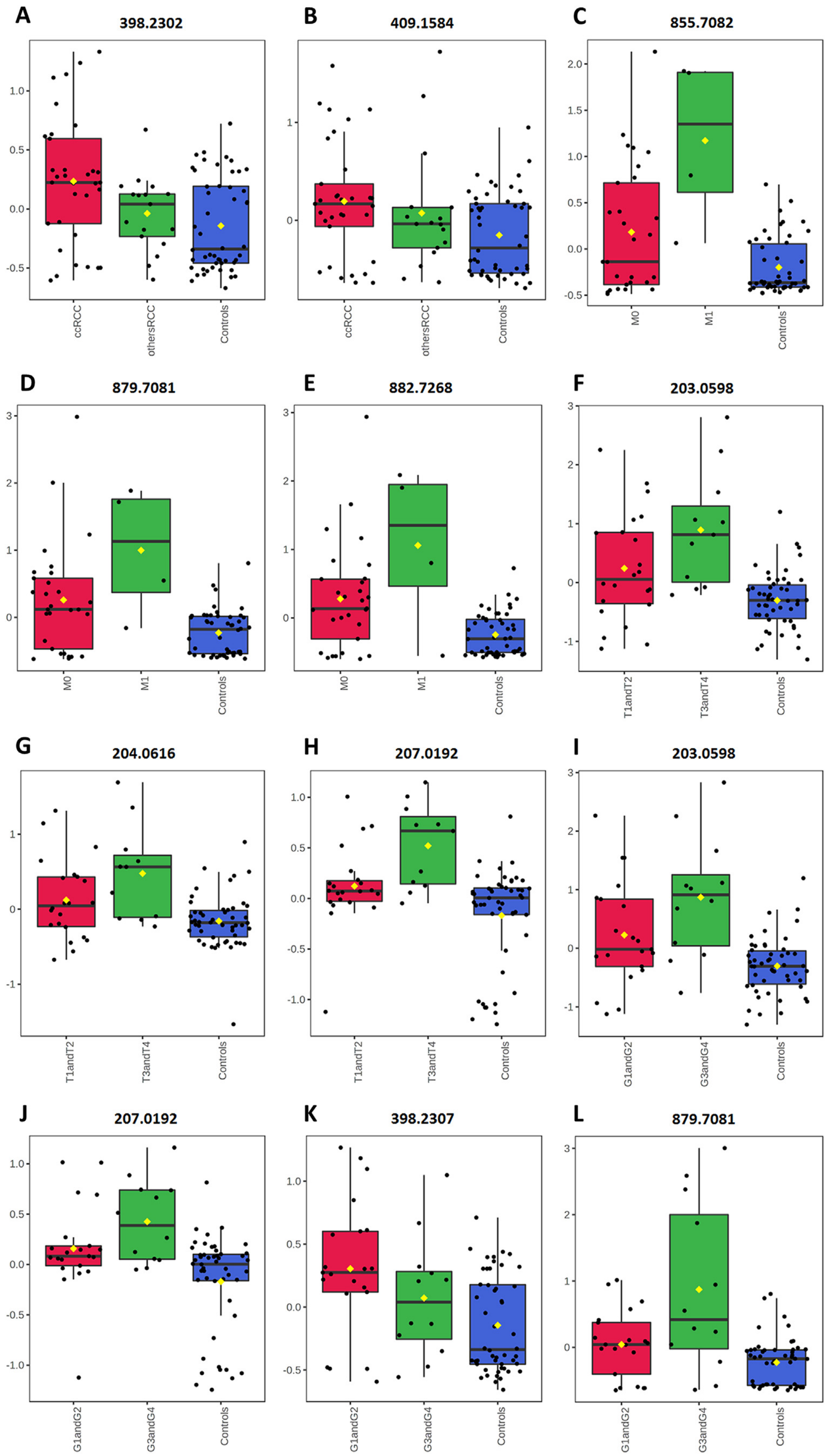

Fig. 3. Box plots for *m/z* values obtained for blood serum samples, distinctive ccRCC and controls: 398.2302 (A), 409.1584 (B), with and without metastases: 855.7082 (C), 879.7081 (D), 882.7268 (E), low stages and high stages: 203.0598 (F), 204.0616 (G), 207.0192 (H), low grade and high grade: 203.0598 (I), 207.0192 (J), 398.2307 (K), 879.7081 (L).
Abbreviations: ccRCC – clear cell renal cell carcinoma, *m/z* – mass to charge ratio.

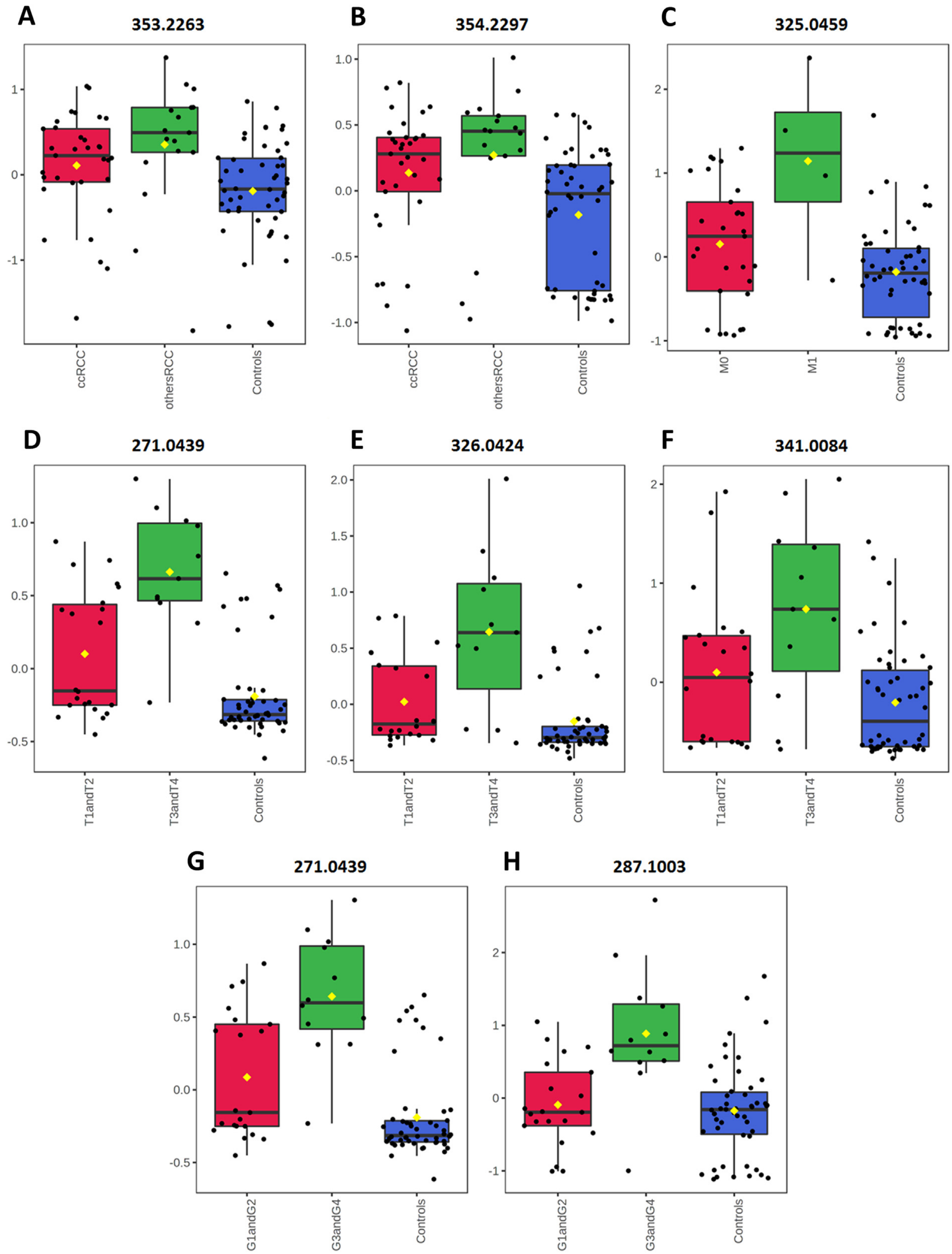

Fig. 4. Box plots for *m/z* values obtained for urine samples, distinctive ccRCC and controls: 353.2263 (A), 354.2297 (B), with and without metastases: 325.0459 (C), low stages and high stages: 271.0439 (D), 326.0424 (E), 341.0084 (F), low grade and high grade: 271.0439 (G), 287.1003 (H).
Abbreviations: ccRCC – clear cell renal cell carcinoma, *m/z* – mass to charge ratio.

Financial disclosure

Scientific work funded by the Polish Ministry of Science and Higher Education, from the budget for science in the years 2016–2020 as a research project within the program "Diamond Grant" (project no. 0184/DIA/2016/45).

The author contribution

Study Design: Adrian Arendowski, Joanna Nizioł, Tomasz Ruman.

Data Collection: Adrian Arendowski, Krzysztof Ossoliński, Anna Ossolińska, Tadeusz Ossoliński, Joanna Nizioł.

Statistical Analysis: Adrian Arendowski.

Data Interpretation: Adrian Arendowski.

Manuscript Preparation: Adrian Arendowski, Krzysztof Ossolioński, Tomasz Ruman.

Literature Search: Adrian Arendowski.

Funds Collection: Adrian Arendowski.

Declaration of competing interest

The authors declare no competing and financial interest.

Acknowledgements

Mr Dominik Ruman is acknowledged for creating MS search engine of chemical compounds.

Appendix A. Supplementary data

Supplementary data to this article can be found online at https://doi.org/10.1016/j.advms.2021.07.003.

References

[1] Bray F, Ferlay J, Soerjomataram I, Siegel RL, Torre LA, Jemal A. Global cancer statistics 2018: GLOBOCAN estimates of incidence and mortality worldwide for 36 cancers in 185 countries. CA A Cancer J Clin 2018;68:394–424. https://doi.org/10.3322/caac.21492.
[2] Chow W-H, Dong LM, Devesa SS. Epidemiology and risk factors for kidney cancer. Nat Rev Urol 2010;7:245–57. https://doi.org/10.1038/nrurol.2010.46.
[3] Moch H. An overview of renal cell cancer: pathology and genetics. Semin Canc Biol 2013;23:3–9. https://doi.org/10.1016/j.semcancer.2012.06.006.
[4] Capitanio U, Bensalah K, Bex A, Boorjian SA, Bray F, Coleman J, et al. Epidemiology of renal cell carcinoma. Eur Urol 2019;75:74–84. https://doi.org/10.1016/j.eururo.2018.08.036.
[5] Müller SA, Pahernik S, Hinz U, Martin DJ, Wente MN, Hackert T, et al. Renal tumors and second primary pancreatic tumors: a relationship with clinical impact? Patient Saf Surg 2012;6:18. https://doi.org/10.1186/1754-9493-6-18.
[6] Yuasa T, Inoshita N, Saiura A, Yamamoto S, Urakami S, Masuda H, et al. Clinical outcome of patients with pancreatic metastases from renal cell cancer. BMC Canc 2015;15:46. https://doi.org/10.1186/s12885-015-1050-2.
[7] Ball Mark W, Bezerra Stephania M, Gorin Michael A, Morgan Cowan, Pavlovich Christian P, Pierorazio Phillip M, et al. Grade heterogeneity in small renal masses: potential implications for renal mass biopsy. J Urol 2015;193:36–40. https://doi.org/10.1016/j.juro.2014.06.067.
[8] Falegan O, Ball M, Shaykhutdinov R, Pieroraio P, Farshidfar F, Vogel H, et al. Urine and serum metabolomics analyses may distinguish between stages of renal cell carcinoma. Metabolites 2017;7:6. https://doi.org/10.3390/metabo7010006.
[9] Mytsyk Y, Dosenko V, Skrzypczyk MA, Borys Y, Diychuk Y, Kucher A, et al. Potential clinical applications of microRNAs as biomarkers for renal cell carcinoma. Cent European J Urol 2018;71:295–303. https://doi.org/10.5173/ceju.2018.1618.
[10] Ngo TC, Wood CG, Karam JA. Biomarkers of renal cell carcinoma. Urol Oncol Semin Orig Investig 2014;32:243–51. https://doi.org/10.1016/j.urolonc.2013.07.011.
[11] Monteiro MS, Carvalho M, de Lourdes Bastos M, de Pinho PG. Biomarkers in renal cell carcinoma: a metabolomics approach. Metabolomics 2014;10:1210–22. https://doi.org/10.1007/s11306-014-0659-5.
[12] Pastore AL, Palleschi G, Silvestri L, Moschese D, Ricci S, Petrozza V, et al. Serum and urine biomarkers for human renal cell carcinoma. Dis Markers 2015;2015:251403. https://doi.org/10.1155/2015/251403.
[13] Gupta A, Nath K, Bansal N, Kumar M. Role of metabolomics-derived biomarkers to identify renal cell carcinoma: a comprehensive perspective of the past ten years and advancements. Expert Rev Mol Diagn 2020;20:5–18. https://doi.org/10.1080/14737159.2020.1704259.
[14] Yang OCY, Maxwell PH, Pollard PJ. Renal cell carcinoma: translational aspects of metabolism and therapeutic consequences. Kidney Int 2013;84:667–81. https://doi.org/10.1038/ki.2013.245.
[15] Rodrigues D, Monteiro M, Jerónimo C, Henrique R, Belo L, Bastos M de L, et al. Renal cell carcinoma: a critical analysis of metabolomic biomarkers emerging from current model systems. Transl Res 2017;180:1–11. https://doi.org/10.1016/j.trsl.2016.07.018.
[16] Dill AL, Eberlin LS, Zheng C, Costa AB, Ifa DR, Cheng L, et al. Multivariate statistical differentiation of renal cell carcinomas based on lipidomic analysis by ambient ionization imaging mass spectrometry. Anal Bioanal Chem 2010;398:2969–78. https://doi.org/10.1007/s00216-010-4259-6.
[17] Arendowski A, Nizioł J, Ossoliński K, Ossolińska A, Ossoliński T, Dobrowolski Z, et al. Laser desorption/ionization MS imaging of cancer kidney tissue on silver nanoparticle-enhanced target. Bioanalysis 2018;10:83–94. https://doi.org/10.4155/bio-2017-0195.
[18] Catchpole G, Platzer A, Weikert C, Kempkensteffen C, Johannsen M, Krause H, et al. Metabolic profiling reveals key metabolic features of renal cell carcinoma. J Cell Mol Med 2011;15:109–18. https://doi.org/10.1111/j.1582-4934.2009.00939.x.
[19] Wettersten HI, Hakimi AA, Morin D, Bianchi C, Johnstone ME, Donohoe DR, et al. Grade-dependent metabolic reprogramming in kidney cancer revealed by combined proteomics and metabolomics analysis. Canc Res 2015;75:2541–52. https://doi.org/10.1158/0008-5472.CAN-14-1703.
[20] Zira AN, Theocharis SE, Mitropoulos D, Migdalis V, Mikros E. 1H NMR metabonomic analysis in renal cell carcinoma: a possible diagnostic tool. J Proteome Res 2010;9:4038–44. https://doi.org/10.1021/pr100226m.
[21] Süllentrop F, Moka D, Neubauer S, Haupt G, Engelmann U, Hahn J, et al. 31P NMR spectroscopy of blood plasma: determination and quantification of phospholipid classes in patients with renal cell carcinoma. NMR Biomed 2002;15:60–8. https://doi.org/10.1002/nbm.758.
[22] Zhang F, Ma X, Li H, Guo G, Li P, Li H, et al. The predictive and prognostic values of serum amino acid levels for clear cell renal cell carcinoma. Urol Oncol Semin Orig Investig 2017;35:392–400. https://doi.org/10.1016/j.urolonc.2017.01.004.
[23] Lin L, Yu Q, Yan X, Hang W, Zheng J, Xing J, et al. Direct infusion mass spectrometry or liquid chromatography mass spectrometry for human metabonomics? A serum metabonomic study of kidney cancer. Analyst 2010;135:2970–8. https://doi.org/10.1039/C0AN00265H.
[24] Zheng H, Ji J, Zhao L, Chen M, Shi A, Pan L, et al. Prediction and diagnosis of renal cell carcinoma using nuclear magnetic resonance-based serum metabolomics and self-organizing maps. Oncotarget 2016;7:59189–98. https://doi.org/10.18632/oncotarget.10830.
[25] Nizioł J, Ossoliński K, Tripet BP, Copié V, Arendowski A, Ruman T. Nuclear magnetic resonance and surface-assisted laser desorption/ionization mass spectrometry-based serum metabolomics of kidney cancer. Anal Bioanal Chem 2020;412:5827–41. https://doi.org/10.1007/s00216-020-02807-1.
[26] Kim K, Aronov P, Zakharkin SO, Anderson D, Perroud B, Thompson IM, et al. Urine metabolomics analysis for kidney cancer detection and biomarker discovery. Mol Cell Proteomics 2009;8:558–70. https://doi.org/10.1074/mcp.M800165-MCP200.
[27] Ganti S, Weiss RH. Urine metabolomics for kidney cancer detection and biomarker discovery. Urol Oncol Semin Orig Investig 2011;29:551–7. https://doi.org/10.1016/j.urolonc.2011.05.013.
[28] Kind T, Tolstikov V, Fiehn O, Weiss RH. A comprehensive urinary metabolomic approach for identifying kidney cancer. Anal Biochem 2007;363:185–95. https://doi.org/10.1016/j.ab.2007.01.028.
[29] Nizioł J, Bonifay V, Ossoliński K, Ossoliński T, Ossolińska A, Sunner J, et al. Metabolomic study of human tissue and urine in clear cell renal carcinoma by LC-HRMS and PLS-DA. Anal Bioanal Chem 2018;410:3859–69. https://doi.org/10.1007/s00216-018-1059-x.
[30] Gao H, Dong B, Liu X, Xuan H, Huang Y, Lin D. Metabonomic profiling of renal cell carcinoma: high-resolution proton nuclear magnetic resonance spectroscopy of human serum with multivariate data analysis. Anal Chim Acta 2008;624:269–77. https://doi.org/10.1016/j.aca.2008.06.051.
[31] Nizioł J, Ossoliński K, Tripet BP, Copié V, Arendowski A, Ruman T. Nuclear magnetic resonance and surface-assisted laser desorption/ionization mass spectrometry-based metabolome profiling of urine samples from kidney cancer patients. J Pharmaceut Biomed Anal 2021;193:113752. https://doi.org/10.1016/j.jpba.2020.113752.
[32] Nizioł J, Copié V, Tripet BP, Nogueira LB, Nogueira KOPC, Ossoliński K, et al. Metabolomic and elemental profiling of human tissue in kidney cancer. Metabolomics 2021;17:30. https://doi.org/10.1007/s11306-021-01779-2.
[33] Jungblut P, Thiede B. Protein identification from 2-DE gels by MALDI mass spectrometry. Mass Spectrom Rev 1997;16:145–62. https://doi.org/10.1002/(SICI)1098-2787(1997)16:3<145::AID-MAS2>3.0.CO;2-H.
[34] Berkenkamp S, Kirpekar F, Hillenkamp F. Infrared MALDI mass spectrometry of large nucleic acids. Science 1998;281:260–2. https://doi.org/10.1126/science.281.5374.260.
[35] Montaudo G, Samperi F, Montaudo MS. Characterization of synthetic polymers by MALDI-MS. Prog Polym Sci 2006;31:277–357.
[36] Gianazza E, Chinello C, Mainini V, Cazzaniga M, Squeo V, Albo G, et al. Alterations of the serum peptidome in renal cell carcinoma discriminating benign and malignant kidney tumors. J Proteomics 2012;76:125–40. https://doi.org/10.1016/j.jprot.2012.07.032.
[37] Jan Sunner, Edward Dratz, Y-Chie Chen. Graphite surface-assisted laser desorption/ionization time-of-flight mass spectrometry of peptides and proteins from liquid solutions. Anal Chem 1995;67:4335–42. https://doi.org/10.1021/ac00119a021.

[38] Abdelhamid HN, Wu H-F. Gold nanoparticles assisted laser desorption/ionization mass spectrometry and applications: from simple molecules to intact cells. Anal Bioanal Chem 2016;408:4485–502. https://doi.org/10.1007/s00216-016-9374-6.

[39] Liu Z, Zhang P, Pyttlik A, Kraus T, Volmer DA. Influence of core size and capping ligand of gold nanoparticles on the desorption/ionization efficiency of small biomolecules in AP-SALDI-MS. Anal Sci Adv 2020;1:210–20. https://doi.org/10.1002/ansa.202000002.

[40] Lai SK-M, Cheng Y-H, Tang H-W, Ng K-M. Silver–gold alloy nanoparticles as tunable substrates for systematic control of ion-desorption efficiency and heat transfer in surface-assisted laser desorption/ionization. Phys Chem Chem Phys 2017;19:20795–807. https://doi.org/10.1039/C7CP04033D.

[41] Ray P, Clément M, Martini C, Abdellah I, Beaunier P, Rodriguez-Lopez J-L, et al. Stabilisation of small mono- and bimetallic gold–silver nanoparticles using calix[8] arene derivatives. New J Chem 2018;42:14128–37. https://doi.org/10.1039/C8NJ02451K.

[42] Abdelhamid HN, Talib A, Wu H-F. One pot synthesis of gold – carbon dots nanocomposite and its application for cytosensing of metals for cancer cells. Talanta 2017;166:357–63. https://doi.org/10.1016/j.talanta.2016.11.030.

[43] Sekuła J, Nizioł J, Misiorek M, Dec P, Wrona A, Arendowski A, et al. Gold nanoparticle-enhanced target for MS analysis and imaging of harmful compounds in plant, animal tissue and on fingerprint. Anal Chim Acta 2015;895:45–53. https://doi.org/10.1016/j.aca.2015.09.003.

[44] Arendowski A, Szulc J, Nizioł J, Gutarowska B, Ruman T. Metabolic profiling of moulds with laser desorption/ionization mass spectrometry on gold nanoparticle enhanced target. Anal Biochem 2018;549:45–52. https://doi.org/10.1016/j.ab.2018.03.016.

[45] Nizioł J, Ossoliński K, Ossoliński T, Ossolińska A, Bonifay V, Sekuła J, et al. Surface-Transfer mass spectrometry imaging of renal tissue on gold nanoparticle enhanced target. Anal Chem 2016;88:7365–71. https://doi.org/10.1021/acs.analchem.6b01859.

[46] Arendowski A, Ossoliński K, Nizioł J, Ruman T. Gold nanostructures - assisted laser desorption/ionization mass spectrometry for kidney cancer blood serum biomarker screening. Int J Mass Spectrom 2020;456:116396. https://doi.org/10.1016/j.ijms.2020.116396.

[47] Arendowski A, Ossolinski K, Niziol J, Ruman T. Screening of urinary renal cancer metabolic biomarkers with gold nanoparticles - assisted laser desorption/ionization mass spectrometry. Anal Sci 2020;36:1521–7. https://doi.org/10.2116/analsci.20P226.

[48] Remily-Wood E, Dirscherl H, Koomen JM. Acid hydrolysis of proteins in matrix assisted laser desorption ionization matrices. J Am Soc Mass Spectrom 2009;20:2106–15. https://doi.org/10.1016/j.jasms.2009.07.007.

[49] Sekuła J, Nizioł J, Rode W, Ruman T. Gold nanoparticle-enhanced target (AuNPET) as universal solution for laser desorption/ionization mass spectrometry analysis and imaging of low molecular weight compounds. Anal Chim Acta 2015;875:61–72. https://doi.org/10.1016/j.aca.2015.01.046.

[50] Niedermeyer THJ, Strohalm M. mMass as a software tool for the annotation of cyclic peptide tandem mass spectra. PLoS One 2012;7:e44913. https://doi.org/10.1371/journal.pone.0044913.

[51] Wishart DS, Feunang YD, Marcu A, Guo AC, Liang K, Vázquez-Fresno R, et al. HMDB 4.0: the human metabolome database for 2018. Nucleic Acids Res 2018;46:D608–17. https://doi.org/10.1093/nar/gkx1089.

[52] Fahy E, Sud M, Cotter D, Subramaniam S. LIPID MAPS online tools for lipid research. Nucleic Acids Res 2007;35:W606–12. https://doi.org/10.1093/nar/gkm324.

[53] Patiny L, Borel A. ChemCalc: a building block for tomorrow's chemical infrastructure. J Chem Inf Model 2013;53:1223–8. https://doi.org/10.1021/ci300563h.

[54] Chong J, Wishart DS, Xia J. Using MetaboAnalyst 4.0 for comprehensive and integrative metabolomics data analysis. Curr Protoc Bioinf 2019;68:e86. https://doi.org/10.1002/cpbi.86.

[55] Ganti S, Taylor SL, Kim K, Hoppel CL, Guo L, Yang J, et al. Urinary acylcarnitines are altered in human kidney cancer. Int J Canc 2012;130:2791–800. https://doi.org/10.1002/ijc.26274.

[56] Tugnoli V, Poerio A, Tosi MR. Phosphatidylcholine and cholesteryl esters identify the infiltrating behaviour of a clear cell renal carcinoma: 1H, 13C and 31P MRS evidence. Oncol Rep 2004;12:353–6. https://doi.org/10.3892/or.12.2.353.

[57] Ackerman D, Tumanov S, Qiu B, Michalopoulou E, Spata M, Azzam A, et al. Triglycerides promote lipid homeostasis during hypoxic stress by balancing fatty acid saturation. Cell Rep 2018;24:2596–605. https://doi.org/10.1016/j.celrep.2018.08.015. e5.

[58] Leja-Szpak A, Pierzchalski P, Goralska M, Nawrot-Porabka K, Bonior J, Link-Lenczowski P, et al. Kynuramines induce overexpression of heat shock proteins in pancreatic cancer cells via 5-hydroxytryptamine and MT1/MT2 receptors. J Physiol Pharmacol Off J Pol Physiol Soc 2015;66:711–8.

[59] Burton C, Ma Y. The role of urinary pteridines as disease biomarkers. Pteridines 2017;28:1–21. https://doi.org/10.1515/pterid-2016-0013.

[60] Kośliński P, Daghir-Wojtkowiak E, Szatkowska-Wandas P, Markuszewski M, Markuszewski MJ. The metabolic profiles of pterin compounds as potential biomarkers of bladder cancer—integration of analytical-based approach with biostatistical methodology. J Pharmaceut Biomed Anal 2016;127:256–62. https://doi.org/10.1016/j.jpba.2016.02.038.

[61] Kim K, Taylor SL, Ganti S, Guo L, Osier MV, Weiss RH. Urine metabolomic analysis identifies potential biomarkers and pathogenic pathways in kidney cancer. OMICS J Integr Biol 2011;15:293–303. https://doi.org/10.1089/omi.2010.0094.

[62] Lario S, Ramírez-Lázaro MJ, Sanjuan-Herráez D, Brunet-Vega A, Pericay C, Gombau L, et al. Plasma sample based analysis of gastric cancer progression using targeted metabolomics. Sci Rep 2017;7:17774. https://doi.org/10.1038/s41598-017-17921-x.